

Pair-breaking effects in the Pseudogap Regime: Application to High Temperature Superconductors

Ying-Jer Kao,^{1,*} Andrew P. Iyengar,² Jelena Stajic,² and K. Levin²

¹*Department of Physics, University of Waterloo, Waterloo, ON, N2L3G1, Canada*

²*James Franck Institute and Department of Physics,
University of Chicago, Chicago, IL 60637, U.S.A.*

(Dated: February 1, 2008)

Abrikosov-Gor'kov (AG) theory, the foundation for understanding pair-breaking effects in conventional superconductors, is inadequate when there is an excitation gap (pseudogap) present at the onset of superconductivity. In this paper we present an extension of AG theory within two important, and diametrically opposite approaches to the cuprate pseudogap. The effects of impurities on the pseudogap onset temperature T^* and on T_c , along with comparisons to experiment are addressed.

Impurity effects in the high temperature superconductors have been the subject of a large body of experimental and theoretical literature concentrating on pair-breaking effects on T_c ^{1,2,3,4}, d -wave density of states effects near $T \approx 0$,^{5,6,7}, local suppressions of the order parameter,^{8,9}, transport effects,¹⁰, and aspects of the superconductor-insulator transition¹¹. Although there are works on the effects of a single impurity in the pseudogap models^{12,13,14,15}, with very few exceptions^{4,16} little theoretical attention has been paid to the interplay between the widely observed cuprate pseudogap and the effects of disorder on pair-breaking. This is a particularly striking omission, given that a major fraction of the superconducting phase diagram¹⁷ is associated with a pseudogap. The goal of the present paper is to establish a formal mean-field structure (analogous to Abrikosov-Gor'kov (AG) theory) that incorporates this pseudogap in computing both T_c and gap onset temperature, T^* , along with other derived properties. Here we address two mean-field approaches (orthogonal in their physics, but similar in their formalism), to the incorporation of the pseudogap: one in which the pseudogap derives from superconductivity itself^{18,19,20} ("intrinsic") and one in which it is "extrinsic", either associated with a hidden order parameter^{21,22}, or with band-structure effects^{23,24}. This intrinsic pseudogap^{18,19} arises from a stronger than BCS attractive interaction which leads to finite momentum pair excitations of the normal state and condensate.

In contrast to BCS theory, in the pseudogap phase there is an excitation gap *present at T_c* , which, at low doping x , remains relatively T -independent for all $T \leq T_c$ ²⁵. This necessarily will affect (i) fundamental characteristics of the superconducting phase as well as (ii) the nature of impurity pair-breaking. Indeed, to support (i), there are strong indications from thermodynamics¹⁷ and tunneling²⁶ experiments that the effects of the normal state pseudogap persist below T_c ²⁷. Evidence in support of (ii) comes from the fact that pseudogap effects appear to correlate with the degree of the T_c suppression in the presence of Zn impurities³. This suppression becomes progressively more rapid as the size of the pseudogap grows.

Both intrinsic and extrinsic models for the pseudogap are associated with a generic set of mean-field equations. It is reasonable to stop at a mean-field level because these materials (in some, but not all respects) do not appear to be strikingly different from BCS superconductors, and because the true critical regime appears to be rather narrow²⁸. Moreover, we believe fluctuation effects around strict BCS theory such as the phase fluctuation model of Emery and co-workers²⁹ are unlikely to explain the often very large separation observed between the gap onset temperature T^* and T_c . It seems more appropriate, thus to search for an improved mean field theory²⁸. Then additional fluctuation effects can be appended as needed.

In this generalized mean field approach, in the clean limit and for $T \leq T_c$, the gap and number equations are given by

$$1 + g_{sc} T \sum_{n,\mathbf{k},\alpha} \frac{\varphi_{\mathbf{k}}^2}{\omega_n^2 + E_{\mathbf{k}}^{\alpha 2}} = 0, \quad (1a)$$

$$n = \frac{1}{2} - T \sum_{n,\mathbf{k},\alpha} \frac{i\omega_n + \epsilon_{\mathbf{k}}^{\alpha} - \mu}{\omega_n^2 + E_{\mathbf{k}}^{\alpha 2}}, \quad (1b)$$

where g_{sc} is the coupling constant for the superconducting order parameter, $\varphi_{\mathbf{k}} = (\cos k_x - \cos k_y)$ is the d -wave symmetry factor, Δ_{sc} represents the superconducting order parameter, and Δ_{pg} the pseudogap which persists in the $T \leq T_c$ phase. Finally, α is a band index, which appears in some microscopic approaches^{21,22} to the extrinsic case. The momentum summation in the extrinsic case is over the reduced Brillouin zone. These equations depend in an important way on the electronic dispersion which differs in the two schemes. In the intrinsic school the fermionic dispersion is characterized by

$$E_{\mathbf{k}}^2 = (\epsilon_{\mathbf{k}} - \mu)^2 + \Delta^2(T), \quad (2a)$$

$$\Delta^2(T) = \Delta_{pg}^2(T) + \Delta_{sc}^2(T), \quad (2b)$$

$$\epsilon_{\mathbf{k}} = \xi_{\mathbf{k}}. \quad (2c)$$

Here $\xi_{\mathbf{k}}$ is the "bare" band structure, taken to correspond to a nearest neighbor tight-binding model. This should

be contrasted with that in the extrinsic school,

$$E_{\mathbf{k}}^{\pm 2} = (\epsilon_{\mathbf{k}}^{\pm} - \mu)^2 + \Delta_{sc}^2(T), \quad (3a)$$

$$\epsilon_{\mathbf{k}}^{\pm} = \pm \sqrt{\xi_{\mathbf{k}}^2 + \Delta_{pg}^2(T)}. \quad (3b)$$

The fermionic dispersions of the two schools differ as a direct consequence of the mechanisms that generate the respective pseudogaps. At the mean field level, a pseudogap due to pairing correlations forms as particles and holes mix to form the fermionic quasiparticles. Those of a spin- or charge- ordered state, though, are particle-particle mixtures. In the regime $T \leq T_c$, where sharp excitations exist, these can be taken as the defining characteristics of “intrinsic” and “extrinsic” models of the pseudogap. Since generally $\mu \neq 0$ away from half-filling, only in the intrinsic school is the pseudogap pinned at the Fermi surface.

The respective properties of the pseudogap lead to equations for its magnitude, which we summarize for $T \leq T_c$, in terms of the particle-particle (χ^{pp}) and particle-hole (χ^{ph}) susceptibilities. For the intrinsic school

$$\chi^{pp}(\mathbf{q}, i\omega_n) = T \sum_{\mathbf{k}, m} \frac{i\nu_m + \epsilon_{\mathbf{k}}}{\nu_m^2 + E_{\mathbf{k}}^2} \frac{\varphi_{\mathbf{k}-\mathbf{q}/2}^2}{i(\nu_m - \omega_n) + \epsilon_{\mathbf{k}-\mathbf{q}}},$$

$$\Delta_{pg}^2 = -T \sum_n \sum_{\mathbf{q} \neq 0} \frac{g_{sc}}{1 + g_{sc} \chi^{pp}(\mathbf{q}, i\omega_n, \Delta)}. \quad (4)$$

Note that χ^{pp} depends^{18,20} on the full excitation gap Δ . Here $\Delta_{pg}(T)$ is associated with the number of finite momentum pair excitations of the condensate. These occur when the strength of the attractive interaction g_{sc} is progressively increased, so that it is larger than that associated with the BCS regime. For the extrinsic school, the counterpart equation is

$$\chi^{ph}(\mathbf{0}, 0, \Delta_{sc}, \Delta_{pg}) = T \sum_{n, \mathbf{k}, \alpha} \frac{\varphi_{\mathbf{k}}^2 (\epsilon_{\mathbf{k}}^{\alpha} - \mu)}{(\omega_n^2 + E_{\mathbf{k}}^{\alpha 2}) \epsilon_{\mathbf{k}}^{\alpha}}$$

$$= -g_{pg}^{-1}, \quad (5)$$

where g_{pg} is the coupling constant for the pseudogap order and the momentum summation is over half of the Brillouin zone. Here we consider the pseudogap with same d -wave structure as the superconducting order.

Figure 1 shows the temperature dependencies of the different energy gaps obtained by solving the complete set of equations in the two pseudogap schools within the underdoped regime. In the intrinsic case T^* marks the gradual onset of the pseudogap, which is associated with bosonic or pair excitations formed in the presence of a stronger-than-BCS attractive interaction. Only at and below T_c does the identification of Δ become precise, so that for this (intrinsic) case we plot an extrapolation of Eqs. 1a, 1b, and 4 to $T \geq T_c$. Figure 1a shows that below T_c the fraction of the bosonic population joining the condensate of zero-momentum pairs ($\propto \Delta_{sc}^2$) increases at the expense of the finite-momentum bosonic fraction

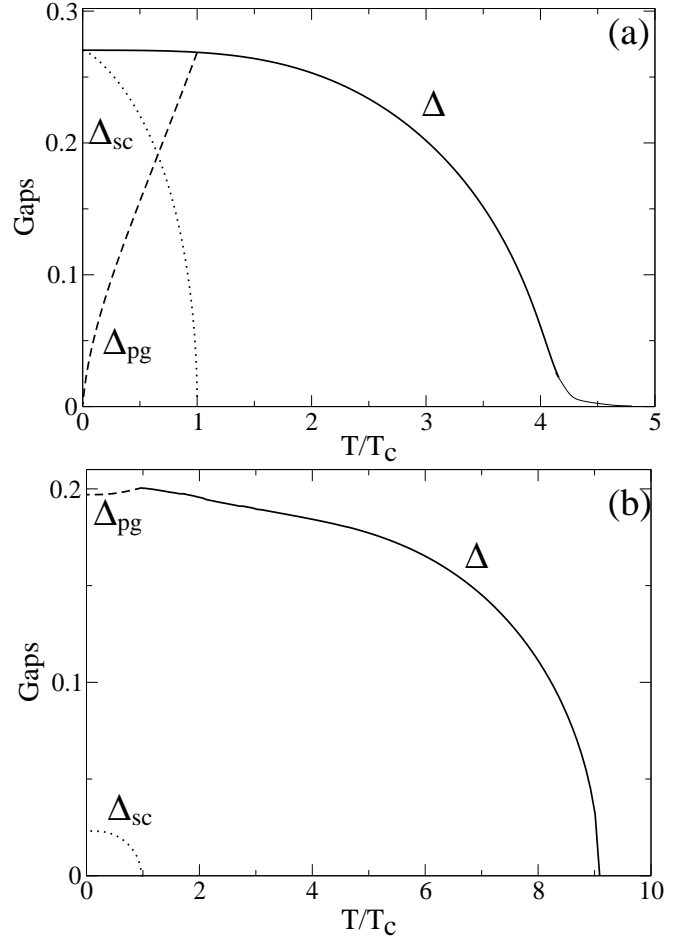


FIG. 1: Energy gaps for intrinsic (a) and extrinsic (b) cases. Solid lines are the total excitation gaps, dotted lines the superconducting order parameters and dashed lines the pseudogaps below T_c . The gaps are in units of $4t_{\parallel}$. The curve for $T \geq T_c$ in (a) represents a rough extrapolation.

($\propto \Delta_{pg}^2$) until the fully condensed ground state is reached. By contrast, for the extrinsic case (Fig. 1b) superconductivity forms on top of a pre-existing excitation gap in the effective band structure which first appears at T^* , the phase transition temperature marking the onset of the extrinsic order.

One can capture the key physics of these two schemes in a reasonably accurate phenomenological approach. The bosonic excitations associated with the mean-field theory¹⁸ of Eqs. (1a), (1b) and (4) lead to the temperature dependence of the pseudogap below the clean limit critical temperature T_{c0}

$$\Delta_{pg}^2(T) \approx \Delta^2(T_{c0}) \left(\frac{T}{T_{c0}} \right)^{3/2}, \quad T \leq T_{c0}. \quad (6)$$

These bosons are, thus, associated with a quasi-ideal Bose gas. By contrast for the extrinsic case, in the well-established pseudogap regime, below T_{c0} , the pseudogap

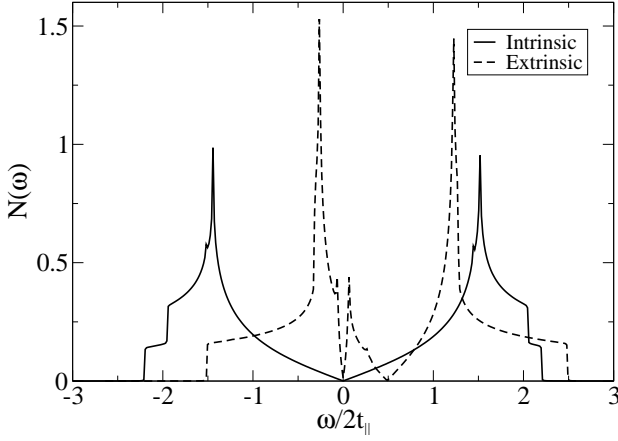


FIG. 2: DOS for intrinsic and extrinsic models at $T = 0$. Only one gap structure appears in the intrinsic DOS, while two distinct gap structures appear in the extrinsic DOS.

is relatively T -independent

$$\Delta_{pg}^2(T) = \Delta^2(T_{c0}), \quad T \leq T_{c0}. \quad (7)$$

Here we define $\Delta(T_{c0}) = \Delta_{pg}(T_{c0})$. In both Eqs. (6) and (7) above, we may view $\Delta(T_{c0})$ as a phenomenological parameter taken from experiment¹⁷. We will adopt this approach here in large part because it provides a more readily accessible theoretical framework for the community, and because it connects more directly with experiment.

The pronounced differences between the fermionic dispersion in these two theoretical schools can be seen from the associated densities of states (DOS) plotted in Fig. 2, which compares the intrinsic and extrinsic models at $T = 0$. In the intrinsic model one sees only one excitation gap feature³⁰ $\Delta = \sqrt{\Delta_{sc}^2 + \Delta_{pg}^2}$ in Fig. 2, centered around the Fermi energy. Van Hove singularities are also apparent here as relatively sharp structures. In contrast, there exist two distinct features for the extrinsic theory. The more prominent pseudogap peaks are centered around $-\mu$, while the superconducting peaks appear around the Fermi energy³¹. Indeed, for this extrinsic case, only in the limit $\mu = 0$ can one readily define an excitation gap Δ as in a conventional superconducting phase³¹, satisfying Eq. (2b). That the superconducting order parameter and pseudogap contribute to separate features in the density of states represents a rather clear signature of this extrinsic pseudogap school. To date, the bulk of experimental tunneling data supports a picture in which there is a single excitation gap feature^{32,33}, although there are some reports of multiple gap structures in c -axis intrinsic tunneling spectroscopy³⁴. At $T = T_c$, the extrinsic superconducting gap closes and the densities of states for the two schools become quite similar, save for the pinning of the gap minimum to the Fermi surface in the intrinsic case.

We turn now to impurity effects which, just as in the BCS case, are not expected to change the formal struc-

ture of our mean field theory. The greatest complication is associated with the impurity-renormalized $\tilde{\Delta}_{pg}$, calculated from all possible diagrammatic insertions of the impurity vertex into the particle-hole and particle-particle susceptibilities [see Eqs. (4) and (5).] A detailed study of these effects in the intrinsic case appears in Ref. 16, although here we will proceed more phenomenologically within both schools. We base the present treatment on analogs of the clean limit mean field gap equations Eqs. (1a) and (1b) with substitutions $\Delta_{sc} \rightarrow \tilde{\Delta}_{sc}$, $\Delta_{pg} \rightarrow \tilde{\Delta}_{pg}$, $\omega_n \rightarrow \tilde{\omega}_n$, and $\mu \rightarrow \tilde{\mu}$. At the phenomenological level the T -dependence of the intrinsic pseudogap is given by

$$\tilde{\Delta}_{pg}^2(T) \approx \tilde{\Delta}^2(T_c) \left(\frac{T}{T_c} \right)^{3/2}, \quad T \leq T_c, \quad (8)$$

and for the extrinsic case,

$$\tilde{\Delta}_{pg}^2(T) \approx \tilde{\Delta}^2(T_c), \quad T \leq T_c. \quad (9)$$

where, in both schools, the excitation gap $\tilde{\Delta}(T_c)$, is presumed to be determined from experiment.

To compute the renormalized frequency $i\tilde{\omega}_n$ and chemical potential $\tilde{\mu}(i\omega_n)$, we follow the usual impurity T -matrix approach. We presume an s -wave short-range impurity potential $V(\mathbf{r}) = u\delta(\mathbf{r} - \mathbf{r}_i)$. The impurity scattering matrix $\hat{T}(\omega_n)$ in Nambu space satisfies the Lippman-Schwinger equation: $\hat{T}(\omega_n) = u\hat{\sigma}_3 \left(1 + \hat{T}(\omega_n) \sum_{\mathbf{k}} \hat{g}(\mathbf{k}, \omega_n) \right)$, where \hat{g} is the impurity-dressed Green's function,

$$\hat{g}(\mathbf{k}, i\omega_n) = \frac{i\tilde{\omega}_n \hat{\sigma}_0 + \mathbf{\Delta}(\mathbf{k}) \hat{\sigma}_1 + (\epsilon_{\mathbf{k}} - \tilde{\mu}) \hat{\sigma}_3}{(i\tilde{\omega}_n)^2 - \tilde{E}_{\mathbf{k}}^2}, \quad (10)$$

Here $\mathbf{\Delta}$ is either the full gap or superconducting order parameter in the intrinsic and extrinsic cases, respectively, and $\hat{\sigma}_i$ are Pauli matrices. Here we suppress the band index in the extrinsic case. Labeling components as $\hat{g} = \sum_i g_i \hat{\sigma}_i$, the regular and anomalous Green's functions are $\tilde{G} = g_0 + g_3$, $\tilde{F} = -g_1$. The frequency and chemical potential are renormalized through impurity self-energy $\hat{\Sigma} = n_i \hat{T}$, and $i\tilde{\omega}_n = i\omega_n - \Sigma_0$, $\tilde{\mu} = \mu - \Sigma_3$, where n_i is the number of impurities per unit cell. We note that the T -matrix for the extrinsic school depends only on the band structure and is independent of the specific type of extrinsic order.

The components of the self-energy are given by

$$\Sigma_0 = \frac{n_i g_0}{(1/u - g_3)^2 - g_0^2}, \quad \Sigma_3 = \frac{n_i (1/u - g_3)}{(1/u - g_3)^2 - g_0^2}, \quad (11)$$

and

$$g_0 = \sum_{\mathbf{k}} \frac{i\tilde{\omega}_n}{(i\tilde{\omega}_n)^2 - \tilde{E}_{\mathbf{k}}^2}, \quad g_3 = \sum_{\mathbf{k}} \frac{\epsilon_{\mathbf{k}} - \tilde{\mu}}{(i\tilde{\omega}_n)^2 - \tilde{E}_{\mathbf{k}}^2}. \quad (12)$$

There is no frequency-dependent self-energy associated with gap renormalization due to d -wave symmetry. Finally, the magnitudes of $\tilde{\Delta}$, $\tilde{\Delta}_{sc}$ and $\tilde{\Delta}_{pg}$ can be obtained

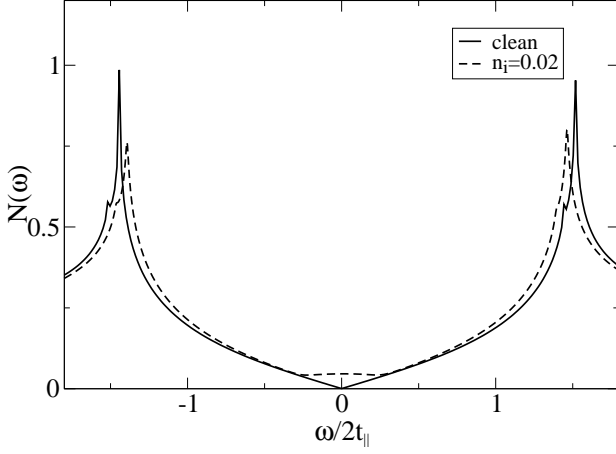


FIG. 3: Intrinsic DOS for the clean and dirty cases at $T = 0$. The DOS is centered around the Fermi energy.

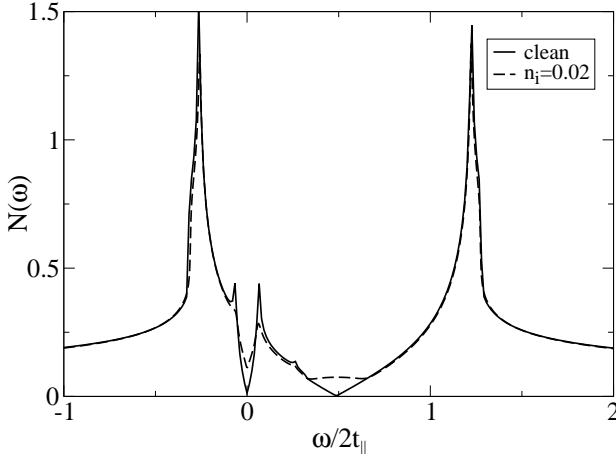


FIG. 4: Extrinsic DOS for the clean and dirty cases at $T = 0$. The DOS is centered around $-\mu$.

using Eqs. (1),(2) and (6), presuming that the excitation gap at T_c is taken from experiment. Here we take the bare lattice dispersion $\xi_{\mathbf{k}} = -2t_{\parallel}(\cos k_x + \cos k_y) - 2t_{\perp} \cos k_z$ so that the dimensionless coupling constant is given by $g/4t_{\parallel}$.

Figures 3 and 4 show the effects of impurities (for unitary scattering) on the density of states at $T = 0$, in the intrinsic and extrinsic cases respectively. As can be seen, particularly for the intrinsic case, impurities decrease slightly the height and separation of the gap peaks [See Fig. 5 below] and fill in the low frequency region, but otherwise their effects are not dramatic. For the extrinsic school, the superconducting gap region is more qualitatively affected by pair-breaking, while the pseudogap peaks remain relatively robust. It can be inferred from these figures that with increasing disorder the differences in the two schools diminish, from the perspective of the density of states, except that the position of the minimum in the extrinsic case is not tied to the Fermi energy. Physical differences, however, remain profound, particu-

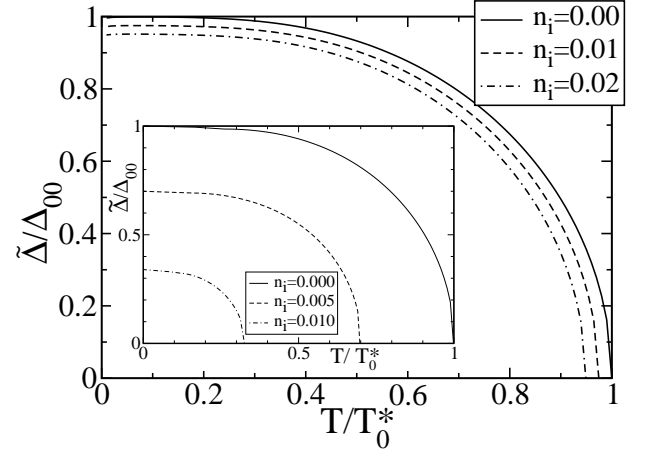


FIG. 5: Temperature dependencies of the full excitation gaps for the intrinsic case at strong ($g/4t_{\parallel} = -1.2$) and weak coupling ($g/4t_{\parallel} = -0.15$, inset), in the unitary limit at different impurity densities. Temperatures are normalized to the clean limit T_0^* and gaps are normalized to the zero-temperature values in the clean limit Δ_{00} .

larly in the electrodynamics^{35,36} of the superconducting phase.

In the remainder of this paper we focus on the behavior of T_c (and T^*) and the appropriate generalization of AG theory in the presence of a pseudogap. For definiteness, we consider Zn doping experiments where we exploit the experimental observation that *the excitation gap $\tilde{\Delta}$ at T_c is relatively unaffected by Zn impurities*¹⁷. We focus here on the unitary limit ($1/u = 0$), which is regarded as relevant to Zn doping in the cuprates.

We begin with the intrinsic school, where the sensitivity of T_c and T^* to the impurity concentration n_i can be studied as a function of a single coupling constant $g = g_{sc}$, which we presume to be unaffected by the addition of impurities. Figure 5 shows the behavior of the excitation gap $\tilde{\Delta}(T)$ vs temperature normalized to its clean limit value, obtained using the impurity-generalized form of Eqs. (1a) and (1b). The figure should be viewed as extending above T_c only in the sense that it provides a reasonable extrapolation³⁷ as well as estimate of T^* . In reality, Fig. 1a indicates that a *crossover* description for the excitation gap at T above T_c is more correct. The main panel corresponds to the strong ($g/4t_{\parallel} = -1.2$) and the inset the weak ($g/4t_{\parallel} = -0.15$) coupling regimes for various values of the impurity density n_i in the unitary limit. In the weak coupling regime, the suppression of the gap is largest, as is the reduction in T^* . In the strong coupling case, the suppression is smaller and at low impurity densities, the curves are very close to those obtained in the clean limit, *indicating smaller pair-breaking effects on the excitation gap and its onset temperature T^** .

Figure 6 shows the way in which impurities suppress the phase coherence temperature T_c at different coupling strengths (in the unitary limit), based on the assumption, supported experimentally³, that the excitation gap

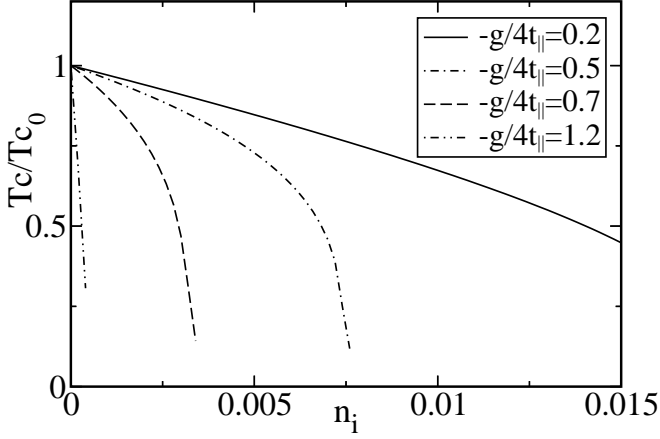


FIG. 6: T_c suppression due to impurities for $1/u = 0$ (unitary limit) in the intrinsic case. The temperatures are normalized to the clean limit T_{c0} .

at the appropriate T_c is relatively independent of impurity concentration. It can be seen that the suppression rate increases as the coupling becomes stronger, or effectively as $\hat{\Delta}(T_c)$ increases. Similar results for the extrinsic case were obtained in Ref. 4. This faster T_c suppression in the strong coupling regime can be understood through a simple physical picture. Impurity scattering will produce states which fill in the gap and eventually destroy superconducting coherence. In the strong coupling (pseudogap) regime, where the normal state already has a gap, fewer impurities are required to restore the system to the “normal” state.

We turn now to calculations which can be directly compared with experiment and plot the normalized slopes of T^* and T_c with respect to increasing Zn concentration, for varying hole concentration x , first for the intrinsic case. To convert from the coupling constant parameter g to x we take as input the experimentally measured values of $\rho_s(x, 0)$ and the measured excitation gap at T_c . Here it is adequate to choose these values corresponding to the pristine case, and presume that Zn doping does not affect the excitation gap at T_c . Figure 7 indicates the initial slope ($1/T_0 dT/dn_i$, where T_0 is the appropriate clean limit temperature) for T^* (dashed line) or T_c (solid line). In the overdoped limit, the theory is asymptotically equivalent to standard AG theory, in which also $T^* = T_c$. For smaller values of x the slope decreases so that T^* is only weakly dependent on impurity concentration. By contrast, the initial T_c slope (solid line) shows a very different hole concentration dependence. As the hole concentration decreases, the slope decreases. However, in the very underdoped regime, where the pseudogap is well established, the curve turns around and rapidly increases. The inset presents a comparison of theory and experiment³ as $\eta = (dT_c/dn_i)/(dT_c/dn_i, x = 0.20)$ vs $z = \Delta_{pg}(T_c)/(\Delta_{pg}(T_c), x = 0.05)$, where the agreement appears to be reasonable. There are fewer systematic studies of impurity-induced changes in T^* ; however, the

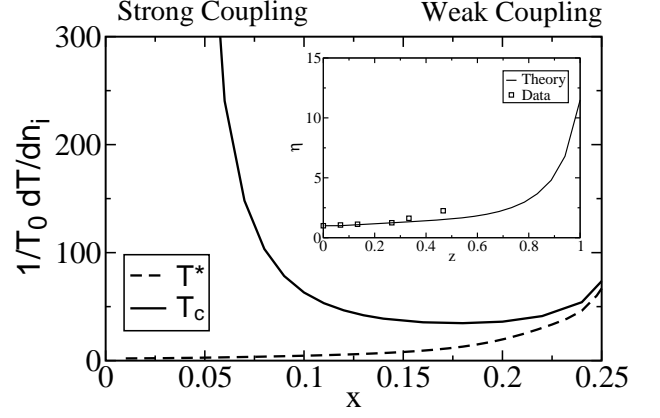


FIG. 7: Initial slopes of T^* and T_c suppression $\frac{1}{T_0} \frac{dT}{dn_i}$ vs doping, in the unitary limit for the intrinsic case. The inset presents a comparison between theory and experimental data from Ref. 3. See text for details.

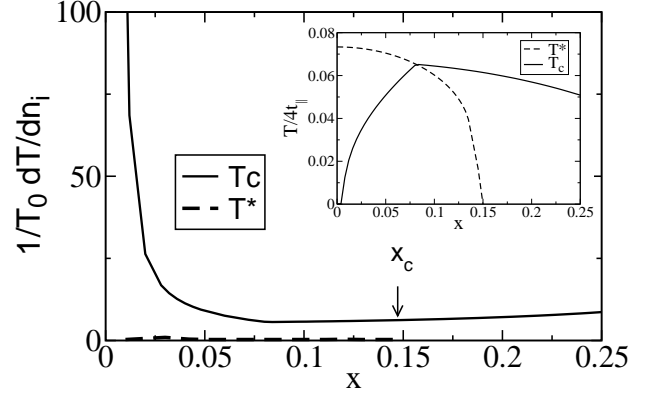


FIG. 8: Initial slopes of T^* and T_c suppression $\frac{1}{T_0} \frac{dT}{dn_i}$ vs doping, in the unitary limit for the extrinsic case. The inset shows the clean phase diagram given by coupling constants $g_{pg}/4t_{||} = -0.4$ and $g_{sc}/4t_{||} = -0.375$. The critical doping x_c where Δ_{pg} vanishes is around 0.15.

small effect found here at low x appears to be compatible with the data.

Finally in Fig. 8 we present the counterpart plots of the initial slopes for T_c and T^* in the extrinsic case. T_c is computed as in the intrinsic case by assuming $\Delta_{pg}(T_c)$ is relatively insensitive to impurities. Impurity renormalizations are determined through Eqs. (11) and (12) while the suppression of T^* is calculated via Eqs. (1b) and (5), extended to include appropriate impurity renormalizations. The inset shows the clean phase diagram which forms the basis for these calculations. Our fit to the published form¹³ of this phase diagram provided values for the coupling constants $g_{pg}/4t_{||} = -0.4$ and $g_{sc}/4t_{||} = -0.375$. To make contact with experiment we chose a parameter set in which T_c/T^* and $n_s/\Delta(0)$ were reasonably well fit to experiment in the underdoped regime. As is similar to the intrinsic case, there is a dramatic increase in the slope of T_c as the insulator is

approached. This increase is associated with the onset of the pseudogap which occurs for $x \leq 0.15$. Above this critical concentration T^* is zero, and the system becomes a conventional dirty BCS superconductor. In this way, the intrinsic and extrinsic schools differ, since for the former at large x , $T^* \rightarrow T_c$.

The theoretical machinery that we have set up has strong similarities to an approach taken by Loram and collaborators²³, extended further to the disordered case^{3,4}. It should be stressed, though, that their approach is a *hybrid* of extrinsic and intrinsic pseudogap theories, where the temperature dependence of the various gap parameters corresponds to the extrinsic case (shown in Fig. 1b), whereas the dispersion and superfluid density corresponds to an intrinsic pseudogap. As shown in this paper, pair-breaking effects on T_c can be successfully addressed at a semi-quantitative level both in intrinsic and extrinsic models⁴. It should be noted that the rather strikingly different sensitivities of T^* and T_c to impurity concentration which are found experimentally, are often taken as an indication that the cuprate pseudogap cannot be intrinsic, i.e., related to the superconductivity, itself. Indeed similar results are found in the presence of magnetic field pair-breaking³⁸ and it should be viewed as one of the fundamental results of this paper that this inference is incorrect. *The differences lie in the fact that an excitation gap is present when T_c is established, but not at T^* , and it is this gap in the density of states that contributes to the stronger pair-breaking effects in T_c .* Indeed, it is precisely this excitation gap which invalidates the results of conventional AG theory. It may be necessary eventually to incorporate an even more local treatment of pair-breaking than that discussed here, but *such a Bogoliubov-de Gennes generalization must include pseudogap effects*. Indeed, the very basis for a more local treatment of impurities² is the observed small coherence lengths, which are at the heart of the present “intrinsic” pseudogap theories¹⁸.

In summary, in this paper we find within two diametrically opposed pseudogap schools, that pseudogap effects at and *below* T_c must play an essential role in pair-breaking. While there is no definitive experiment to distinguish between these two schools, we have argued elsewhere^{35,36} that the intrinsic dispersion leads to smaller and more benign modifications of BCS theory. In both theoretical approaches, the rather robust behavior for T^* and the associated excitation gap in the underdoped regime, found in the presence of impurities may be associated with the widely observed superconductor-insulator transition¹¹. Superconducting coherence is more readily destroyed than is the excitation gap (and T^*), thereby leading to an insulating state when T_c is suppressed to zero, in much the same way as in the presence of applied magnetic fields³⁸. While there are clear differences, seen particularly in electrodynamic calculations^{35,36} (as well as density of states effects) between the intrinsic and extrinsic pseudogap schools, the impurity sensitivities of T_c within these two different approaches are quite similar, and reasonably consistent with experiment. This similarity derives from the fact that both mean field theoretic calculations of T_c have a general BCS-like character, except for the presence of a (pseudo) gap at the onset of superconductivity. For T^* the differences are more apparent in the overdoped regime and this, in turn, reflects the fact that $T^* \rightarrow 0$ in one case (extrinsic), whereas $T^* \rightarrow T_c$ in another (intrinsic). In this paper we have set the stage for a computation of transport properties which require as an essential input, an understanding of impurity effects. The generalization of AG theory presented here should help to clarify the important role played by pseudogap effects, at T_c and their relation to impurity-induced pair-breaking.

We acknowledge very useful conversations with Q. Chen. This work was supported by NSF-MRSEC Grant No. DMR-9808595 (YK, JS, AI, KL) and by NSERC of Canada and Research Corporation (YK).

-
- * Electronic address: y2kao@uwaterloo.ca
- ¹ R. J. Radtke, S. Ullah, K. Levin, and M. R. Norman, Phys. Rev. B **46**, 11975 (1992).
 - ² M. Franz, C. Kallin, A. J. Berlinsky, and M. I. Salkola, Phys. Rev. B **56**, 7882 (1997).
 - ³ J. L. Tallon, C. Bernhard, G. V. M. Williams, and J. W. Loram, Phys. Rev. Lett. **79**, 5294 (1997).
 - ⁴ G. V. M. Williams, E. M. Haines, and J. L. Tallon, Phys. Rev. B **57**, 146 (1998).
 - ⁵ C. Pépin and P. A. Lee, Phys. Rev. B **63**, 054502 (2001).
 - ⁶ T. Sentil and M. Fisher, Phys. Rev. B **60**, 6893 (1999).
 - ⁷ W. A. Atkinson, P. J. Hirschfeld, A. H. MacDonald, and K. Ziegler, Phys. Rev. Lett. **85**, 3926 (2000).
 - ⁸ M. E. Zhitomirsky and M. B. Walker, Phys. Rev. Lett. **80**, 5413 (1998).
 - ⁹ S. H. Pan et al., Nature **413**, 282 (2001).
 - ¹⁰ A. Durst and P. A. Lee, Phys. Rev. B **62**, 1270 (2000).
 - ¹¹ Y. Fukuzumi, K. Mizuhashi, K. Takenaka, and S. Uchida, Phys. Rev. Lett. **76**, 684 (1996).
 - ¹² H. V. Kruis, I. Martin, and A. V. Balatsky, Phys. Rev. B **64**, 054501 (2001).
 - ¹³ J.-X. Zhu, W. Kim, C. S. Ting, and J. P. Carbotte, Phys. Rev. Lett. **87**, 197001 (2001).
 - ¹⁴ Q.-H. Wang, Phys. Rev. Lett. **88**, 057002 (2002).
 - ¹⁵ D. K. Morr, Phys. Rev. Lett. **89**, 106401 (2002).
 - ¹⁶ Q. J. Chen and J. R. Schrieffer, Phys. Rev. B **66**, 014512 (2002).
 - ¹⁷ J. L. Tallon and J. W. Loram, Physica C **349**, 53 (2001).
 - ¹⁸ I. Kosztin, Q. Chen, B. Janko, and K. Levin, Phys. Rev. B **58**, R5936 (1998).
 - ¹⁹ Q. Chen, I. Kosztin, B. Janko, and K. Levin, Phys. Rev. Lett. **81**, 4708 (1998).
 - ²⁰ B. Janko, J. Maly, and K. Levin, Phys. Rev. B **56**, R11407 (1997).
 - ²¹ S. Chakravarty, R. B. Laughlin, D. K. Morr, and C. Nayak, Phys. Rev. B **63**, 094503 (2001).

- ²² C. Castellani, C. DiCastro, and M. Grilli, Phys. Rev. Lett. **75**, 4650 (1995).
- ²³ J. W. Loram et al., J. Supercond. **7**, 243 (1994).
- ²⁴ P. Nozieres and F. Pistolesi, Eur. Phys. J. B **10**, 649 (1999).
- ²⁵ M. R. Norman, M. Randeria, H. Ding, and J. C. Campuzano, Phys. Rev. B **57**, 11093 (1998).
- ²⁶ G. Deutscher, Nature **397**, 410 (1999).
- ²⁷ Q. J. Chen, K. Levin, and I. Kosztin, Phys. Rev. B **63**, 184519 (2001).
- ²⁸ V. Geshkenbein, L. Ioffe, and A. Larkin, Phys. Rev. B **55**, 3171 (1997).
- ²⁹ V. J. Emery and S. A. Kivelson, Nature **374**, 434 (1995).
- ³⁰ In the intrinsic model, the distinction between the superconducting order parameter and the pseudogap below T_c can only be observed through the different lifetime of the condensate and the finite-momentum excitations. See Ref 27.
- ³¹ W. Kim, J.-X. Zhu, J. P. Carbotte, and C. S. Ting, Phys. Rev. B **65**, 064502 (2002).
- ³² C. Renner, B. Revaz, K. Kadowaki, I. Maggio-Aprile, and O. Fischer, Phys. Rev. Lett. **80**, 3606 (1998).
- ³³ N. Miyakawa, J. Zasadzinski, L. Ozyuzer, P. Guptasarma, D. G. Hinks, C. Kendziora, and K. E. Gray, Phys. Rev. Lett. **83**, 1018 (1999).
- ³⁴ V. M. Krasnov et al., Phys. Rev. Lett. **84**, 5860 (2000).
- ³⁵ J. Stajic, A. Iyengar, K. Levin, B. R. Boyce, and T. Lemberger, cond-mat/0205497.
- ³⁶ A. P. Iyengar, J. Stajic, Y.-J. Kao, and K. Levin, cond-mat/0208203.
- ³⁷ J. Maly, B. Janko, and K. Levin, Phys. Rev. B **59**, 1354 (1999).
- ³⁸ Y.-J. Kao, A. P. Iyengar, Q. J. Chen, and K. Levin, Phys. Rev. B **64**, 140505 (2001).